Physica Scripta. Vol. T22, 228–237, 1988.

Summary of the Physics in Traps Panel

Chairman and Editor

Robert S. Van Dyck, Jr.

Department of Physics, University of Washington, Seattle, Washington 98195, USA

Panelists

Hans A. Schuessler[1], Randall D. Knight[2], Daniel Dubin[3], William D. Phillips[4], and Greg Lafyatis[5]

[1]Department of Physics, Texas A&M University, College Station, TX 77843 USA; [2]Department of Physics, The Ohio State University, Columbus, OH 43210, USA; [3]Department of Physics, University of California, San Diego, La Jolla, CA 92093, USA; [4]MET, Room B258, National Bureau of Standards, Gaithersburg, MD 20899, USA; [5]Department of Physics, Massachusetts Institute of Technology, Cambridge, MA 02139, USA

Received August 25, 1987; accepted September 18, 1987.

Abstract

The "Physics in Traps" panel speculates on possible experiments for high precision mass spectroscopy, the use of recoil ions, applications to laboratory astrophysics, potential condensed matter experiments, and new ideas for optical and magnetic traps for neutral particles.

1. Introduction

The possibilities for interesting physics experiments which can be done in particle traps seems to be growing at a very rapid rate. In the last several years, we have seen trapped ion experiments on atomic spectroscopy, charge transfer, chemical reactions, electron-ion recombination, fundamental constants, lifetimes, non-neutral plasmas, mass spectroscopy, and photodetachment as well as tests of fundamental symmetries and theories (such as quantum electrodynamics, relativity, spatial isotropy and particle-antiparticle comparisons). In the future, we will see experiments on liquid-solid phase transitions for ion clouds, stored-ion and neutral-atom frequency standards, spectroscopy on highly-charged hydrogen-like ions (i.e., fine structure, hyperfine structure, Lamb shifts, . . .), spectroscopy of neutral antimatter, just to name a few. A number of these possibilities have been addressed in the following sections by the members of the panel.

2. High precision mass spectroscopy in a penning trap

Robert S. Van Dyck, Jr.

For my contribution, I will concentrate on the d.c. Penning trap as the ideal mass spectrometer. The advantages of this device are inherent in the very small ion samples required, the very long containment times which are possible, the non-destructive detection techniques which can be used, the negligible interactions with background gases, and the easily controlled electric and magnetic fields whose effects can be accurately accounted for in ion cyclotron measurements.

The basic device developed at the University of Washington is the compensated Penning trap [1] which consists of precision-machined quadrupole ring and end cap electrodes in addition to special guard rings which compensate the trapping potential, V_0, thus making the trap very harmonic over a large working volume. Custom-built, cryogenically cooled, amplifiers combined with high-Q tuned circuits allow us to observe as small as one ion at a time. In general, a charge isolated in such a trap sees an electric restoring force along the axis of symmetry, thus producing a simple harmonic motion at ν_z which can be driven by an appropriate r.f. electric field. As usual, radial confinement is produced by a strong magnetic field (≈ 50 kG), applied along the same axis, thus generating the cyclotron motion at ν_c' which is inversely related to the ion's mass. In addition, the axial magnetic field crossed into the anti-restoring radial electric field produces a very slow magnetron drift at ν_m, thus completing the composite cycloid motion.

The detection scheme consists of driving the axial motion and mixing the resulting signal with the original drive which is appropriately attenuated and phase shifted. In this way, we generate an error signal, which can be used in a feedback loop (via the d.c. ring-end cap potential) to generate the sensitive frequency shift detector [2]. Due to various perturbations which arise from the residual inhomogeneity of d.c. and r.f. electromagnetic fields, we find that magnetron and cyclotron motions can each be observed by this particular detection scheme. Figure 1 illustrates a typical well-resolved proton cyclotron resonance in which the applied cyclotron power causes a very large shift in the axial resonance. Prior to sweeping in either direction, a strong re-centering of the particles is required. The ± 0.1 ppb precision shown in this resonance (and seen in many others) may become routine for all trapped ions with today's homogeneous superconducting magnets and stable d.c. voltage supplies.

Table I lists several experiments in progress which utilize singly-charged particles in a Penning trap for very high precision determinations of fundamental constants. Probably, the most notable of these (as reported in this conference by H. Dehmelt) is the measurement [3] of the electron and positron g-factors to an accuracy of 4 parts in 10^{12}. In a similar experiment, $m(e^+)/m(e^-)$ has been determined [4] to one part in 10^7, but with the potential accuracy of 1 ppb.

Another fundamental constant listed in Table I is the proton-electron mass ratio, determined to an accuracy of 20 ppb. Here, we compare cyclotron frequencies of particles of opposite charge which are subject to potential systematic effects because of possible electrostatic position-shifts within

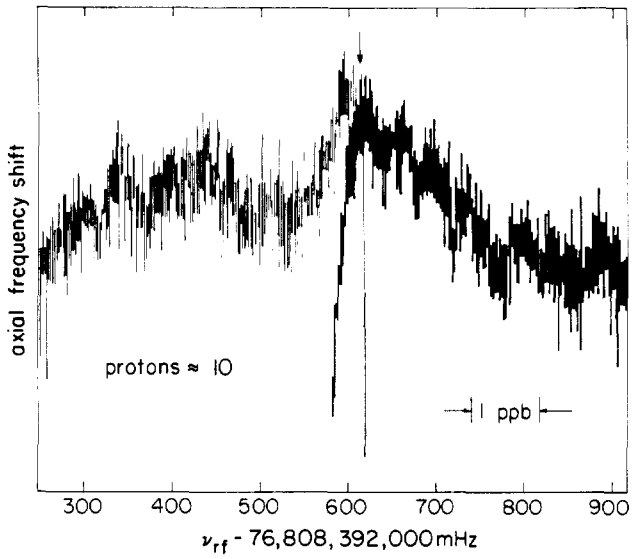

Fig. 1. Proton cyclotron resonance. Large r.f. drives tend to cause sharp axial shifts when the resonance is excited. Here, the power is removed as soon as the resonance became apparent. Subsequently, strong re-centering of the ion cloud is required before the next trace can be made. Resolution is $\approx \pm 0.1$ ppb.

the non-uniform magnetic field. A new device called the variable magnetic bottle [5] allows the quadratic field dependence to be removed, thus reducing a previously large systematic error. We anticipate future research will improve on this comparison by a factor of 10.

Yet another application listed in Table I is the measurement of the deuterium ion mass with respect to the proton's mass. The bare neutron mass is given by $m_n = M(^2H^+) + B_e - m_p$, where $B_e = 2.388\,176\,3(24) \times 10^{-3}$ amu is the deuteron binding energy measured by Greene *et al.* [6]. Thus, it follows that m_n/m_p can be determined from a measurement of $M(^2H^+)/m_p$. An improvement in the γ-ray wavelength measurement to an accuracy of 40 ppb would allow one to obtain a relative precision in m_n/m_p of 0.14 ppb (assuming cyclotron resonances for both protons and deuterium ions are each measured to 0.1 ppb accuracies).

An ongoing project now at 3 different laboratories (at the University of Washington, MIT, and the University of Mainz) is the high precision measurement of the $^3H^+$–$^3He^+$ mass difference in the compensated Penning trap. This difference can be obtained, for instance, from $1 - \nu_c(^3H^+)/\nu_c(^3He^+)$, which then allows the tritium β-decay endpoint energy E_0 to be determined. It should be noted that Lippmaa has simultaneously trapped both $^3H^+$ and $^3He^+$ and successfully measured [7] their mass difference in a commercial spectrometer (with cubic trap) to ≈ 1 part in 10^4. The significance of this measurement arises from the fact that tritium is a low energy beta emitter and its endpoint energy can be accurately determined by looking at the electron's decay spectrum. The major goal of this research is the determination of the antineutrino's rest mass, m_ν. To all the experiments which are involved in the tritium β-decay measurements, the major benefit of having a more precise value for E_0 is either to reduce the number of fitted parameters (and thus the final uncertainty in m_ν) or as a systematic check on the experiments.

Table I. *High precision measurements of fundamental constants using singly-charged particles*

Charge(s)	Significance	Present accuracy	Anticipated accuracy
e^-	g-factor	4×10^{-12}	1×10^{-13}
e^+	g-factor	4×10^{-12}	1×10^{-13}
e^-, e^+	$m(e^+)/m(e^-)$	1×10^{-7}	1×10^{-9}
p^+	m_p/m_e	2×10^{-8}	1×10^{-9}
$^2H^+$	m_n/m_p	1.4×10^{-8}	2×10^{-10}
$^3H^+$, $^3He^+$	$M(^3H) - M(^3He)$	2×10^{-4}	2×10^{-5}
$\bar{p}$	$m_{\bar{p}}/m_p$	$\approx 5 \times 10^{-5}$	1×10^{-9}

Another experiment, also described at this conference, is the proposed measurement of the antiproton mass to the proton mass. An international collaboration headed by G. Gabrielse at the University of Washington along with physicists at the University of Mainz and Fermilab recently captured antiprotons in a simple Penning trap for the first time [8]. The success in slowing down and holding $\bar{p}$ at low energies (< 1 keV) in an ion trap opens up a number of possibilities, but the first experiment being pursued is the measurement of $m_{\bar{p}}/m_p$, which will likely improve the present accuracy [9] by 4–5 orders of magnitude. This will yield an extremely precise test of CPT invariance using baryons.

At this point, we note that the Penning trap is *not* limited to singly charged ions. We have found that by reflecting the electron beam back upon itself, we can ionize background (and adsorbed) gases whose final charge state is limited only by the energy of the electron beam. Typically with ≈ 600 eV electrons, we have observed for example $^{14}N^{5+}$, $^{12}C^{6+}$, $^{16}O^{6+}$, and $^{19}F^{4+}$. As far as the observed axial signal is concerned, assuming we drive the charge(s) as hard as possible without picking up appreciable anharmonic terms in the potential (which destroy one's resolution in frequency space), one can show that the observable signal is linear in the number of ions trapped and in the charge state. Here, we list a few advantages for using the highest convenient charge state for mass ratio measurements:

- It is easy to strip electrons from atoms until $m/q < 3$ (where protons have $m/q = 1$), thus assuring that ν_z and ν_c' will remain reasonably high (for a given V_0) without any substantial change in the magnitude of ν_m.
- Signal increases linearly with charge for a given oscillation amplitude, thus yielding a larger maximum undistorted signal.
- Coupling to the external tuned circuit goes as q^2 and thus response time and cooling rates are enhanced.
- Easy checks on systematics can be done by varying the charge state of a specific type of atom, for instance we can measure $M(C^{n+})/m_p$ for $n = 1, \ldots, 6$.

Now consider the mass ratios: $M(^{15}N^{7+})/m_p$ and $M(^{14}N^{7+})/m_p$. The cyclotron frequency of each nitrogen ion is thus on the order of one half the proton's cyclotron frequency. Another of the advantages is the 49 times stronger coupling to the external tuned circuit (compared to the coupling for a singly charged nitrogen ion) and the 7 times larger absolute signals which can be detected per ion. The interesting application is the determination of α, the fine structure constant. If we define $\Delta m = M(^{14}N^{7+}) - M(^{15}N^{7+}) + m_n$, then, one can show that

$$\alpha^2 = 2R_\infty \frac{m_p}{m_e}\left(\frac{\Delta m}{m_p}\right)\lambda^* \qquad (1)$$

where λ^* is the wavelength of a γ-ray (corrected for nuclear recoil) having energy equal to the neutron binding energy in

^{15}N (≈ 10.85 MeV). Thus, assuming that λ^* and $\Delta m/m_p$ can both be determined to better than 0.1 ppm, then α can be determined to $\approx 1 \times 10^{-7}$ which is competitive with other determinations [10] of α. Since Δm is ≈ 0.01 amu, this means that the absolute uncertainty allowed in each ion mass ratio is 1×10^{-9} amu out of a possible 15 amu. The experiment must therefore yield a relative precision in each cyclotron frequency on the order of 8 parts in 10^{11}. Even at this level of accuracy, the experiment is worth doing since it provides a check on the measurement of α by a completely different method, tied only to the standard second.

Finally, another application involving highly charged ions is the measurement of $M(U^{91+})/m_p$ and $M(U^{92+})/m_p$. A single fully stripped uranium ion is equivalent to 92 singly charged, mass 2.6, particles in the trap without many of the systematic errors associated with 92 charged particles. The significance of "weighing" such a heavy fully stripped ion and its hydrogen-like counterpart is that, upon correcting for the known rest mass of the electron, one can determine the binding energy of the single added electron (which is ≈ 138 keV). Using the known Dirac theory of ionization potentials for hydrogen-like ions, one can then determine the Lamb shift in the $1s$ ground state. For uranium, this shift is expected to be $\approx 8\times$ larger than the Lamb shift in the $2s$ state or ≈ 0.5 keV. Since the mass of this ion is ≈ 220 GeV, a 10% measurement of the Lamb shift would require a 0.16 ppb accuracy in each mass ratio. This may turn out to be relatively easy, and such measurements in these high-Z systems represent very interesting tests of QED in a strong Coulomb field.

This work is supported by the U.S. National Science Foundation under Grant No. PHY87-05397.

3. Determination of the magnetic moment of the bound electron using recoil ions in an ion trap

Hans A. Schuessler

Our measurement of the magnetic moment of stored $^4He^+$ ions has established a high precision method for determining the magnetic moment of the bound electron [11]. As an extension of this experiment, we plan to apply a similar approach to study highly charged hydrogenic ions stored in a radio-frequency (RF) trap in order to more closely examine the predictions of relativistic and quantum electrodynamic (QED) theories. Challenging questions in this context are how the relativistic motion of the bound electron in the vicinity of a high charge (which certainly changes the dressing of virtual photons of the electron) will influence its magnetic moment and can relativistic and QED theories account for all of the changes. As a reminder, in such an experiment what one measures by RF spectroscopy is the g-factor of the bound electron, called g_J, relative to the g-factor of the free electron. This is of course unity plus the relativistic Breit term which varies as $(Z\alpha)^2/3$ and the first radiative term which comes in as $\alpha(Z\alpha)^2/4\pi$. Higher order terms [12] can also be considered later. Because of the Z^2 dependence of the correction terms, one can clearly see the advantage of performing the experiment on highly charged recoil ions.

3.1. *Principle of the measurement of the magnetic moment*

The apparatus has been set up on-line to the heavy ion accelerator UNILAC at GSI in Darmstadt. A recoil ion source, consisting of either a parallel plate extraction region, or an electrostatic ion trap is located in the high energy heavy ion beam and highly charged recoil ions [13] with a few eV of energy are produced at millitorr pressures. In order to do precision experiments, the highly charged ions must be transported into ultrahigh vacuum so that they live long enough to perform the measurement. This is accomplished by using ion optics for extraction and a Wien filter for charge-state selection. Continuous dynamical trapping will be used and is unique to the RF trap and the combined trap. It should allow us to almost fill the ion trap to the space charge limit of about 10^7 ions. In dynamical trapping, use is made of the pulsed recoil ion production which is caused by the time structure of the primary UNILAC beam. Alternately, a sequential bunching of the recoil ions can be carried out at any frequency when the electrostatic recoil-ion source is employed. The basic idea is to inject the slow recoil ions at the optimum phase of the driving voltage. We have shown theoretically [14] that the RF ion trap will accept externally injected ions only during a narrow phase interval which is centered around π for injection through the midpoint of the ring electrode and near $\pi/2$ for injection through the apex of one of the end cap electrodes.

An essential requirement for the experiment is that the electron, bound to the highly charged ion, be spin polarized in a magnetic field. With optical pumping techniques not available in the X-ray region, one way of obtaining a spin polarized state is to prepare the electron spin orientation externally and then transfer the electron to the ion in a charge transfer collision. This is effected with an atomic hydrogen beam which is state selected in a hexapole magnet and injected into the ion trap. It is well known [15] that electron transfer from hydrogen atoms to highly charged low energy ions occurs into a narrow range of excited n-states which quickly decay by direct and cascading electric dipole transitions to the ground state. In the present experiment, however, an additional feature arises since initially a coherent spin state is produced. The electron spin polarization is fully preserved even after multistep cascading to the ground state and with spin orbit interaction present in all participating states. Our recent calculations [16] confirm the intuitive argument that the electric dipole interaction is spin preserving.

The last step in the experiment is to monitor the changes in the bound electron polarization when a resonant RF field is applied. This is achieved by a second charge transfer process for which the final state of the ion is spin dependent. According to Fermi statistics, the second transferred electron, which has the same spin orientation as the first, is excluded from the $1s$-state and ends up in the $2s$-state unless the RF transitions have flipped the orientation of the first electron. The reduction in number of such unique stretched momentum states serves, analogous to a Stern Gerlach experiment, as a means to detect the spin resonance.

3.2. *Status of the experiment*

The main parts have been constructed and also assembled except for the state selected atomic hydrogen beam. The recoil ion source yields ample fluxes of highly charged ions. The transfer of the bunched ion beam and its subsequent trapping are of crucial importance. For high extraction efficiency, the slow recoil ions are accelerated to 2 keV. Then,

now reasonably complete. With higher charge states one gets into emission lines seen in higher temperature plasmas, such as the solar corona as well as fusion plasmas. In the latter case in particular, ion lifetimes are important since these emissions represent major energy losses. Until now, the problem has been one of how to produce a relatively large number of multi-charged ions in the trap. This problem is beginning to be resolved with approaches such as the use of recoil ions, synchrotron radiation ionization, and external loading from ion beams.

Charge exchange is another important area of laboratory astrophysics to which ion traps have begun to make a significant contribution. This is particularly important in that traps can provide cross-section data at low energies, and in this regard ion traps and ion beams are seen as being complementary. One topic of active interest is charge exchange with atomic hydrogen. These experiments are by no means easy since one needs a separate atomic hydrogen beam, but they are significant because most astrophysical hydrogen is atomic rather than molecular. An example of this work is Church's measurements of charge exchange for O^{2+} and O^{3+} with atomic hydrogen [19]. This work provided an important confirmation of theoretical calculations.

In other charge exchange work, both Prior [20] and Church [21] have trapped, from recoil ions, all charge states of neon up to fully stripped Ne^{10+}, and they have measured charge transfer with the parent neutral species. This work is likely a harbinger of things to come, since ion traps provide a convenient and relatively unique means to work with low-energy, multi-charged ions.

Ion-molecule chemistry is also a collision process of paramount importance in understanding the interstellar medium; Dunn's group has been particularly active in this field [22]. This type of chemistry is normally done near or above room temperature with plasma sources, ion beams, etc. However, the interstellar medium is characterized by a temperature of order 10 K. Reaction rate data needed to model the chemistry have often been extrapolated from measurements at much higher temperatures, but the validity of this procedure has been questioned. Dunn's group has begun to measure rates at 10–20 K in a Penning trap. They have looked at both radiative association, as in $CH_3^+ + H_2 \rightarrow CH_5^+ + h\nu$, and also rearrangement reactions, such as the important protonation reaction $NH_3^+ + H_2 \rightarrow NH_4^+ + H$. For this latter reaction, the rate rises rapidly with temperature for $T > 200$ K, and extrapolation to very low temperatures would imply a negligible rate. In fact, Dunn's measurements show that the rate reaches a minimum at $T \approx 50$ K and begins to rise again at lower temperatures. The rate at 10 K is thus several orders of magnitude larger than might have been anticipated from high temperature data alone.

A recent and interesting new topic is that of ion clusters. The work so far has been done in commercial ion cyclotron resonance cells, which are simple Penning traps but which provide rapid, high-resolution mass spectra by Fourier transform techniques. A focused, pulsed laser is used to ablate material from a solid target just outside the cell. For some materials, particularly semiconductors, both positive and negative clusters are formed and trapped as the plasma expands through the cell and recombines. In work on carbon by Knight and colleagues [23], cluster ions containing as many as thirty atoms have been trapped. Figure 3 shows

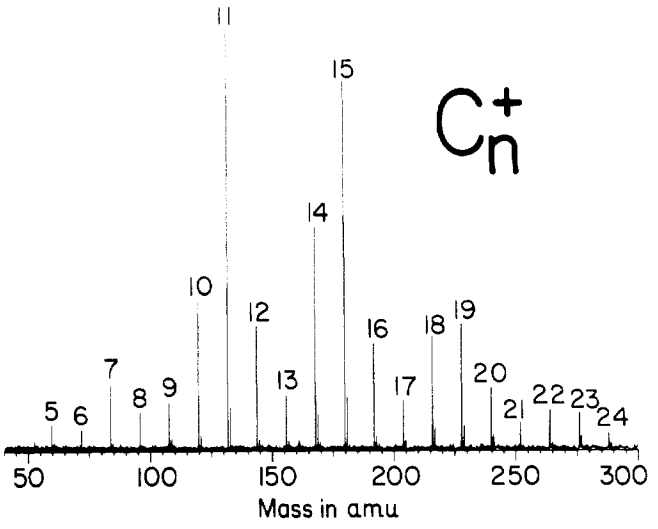

Fig. 3. Fourier transform ion cyclotron resonance mass spectrum of positive carbon cluster ions, showing cluster sizes up to 24 atoms. Note that clusters containing a single ^{13}C atom are clearly resolved.

a representative mass spectrum of stored positive carbon cluster ions. Note the regular pattern of four seen in maxima repeating at 7, 11, 15, 19, and 23. This pattern cannot be destroyed, indicating that some type of "magic numbers" may be involved.

The astrophysical interest lies in the fact that many interstellar molecules are thought to be long carbon chains or other structures of carbon. Thus both the structure and the chemistry of clusters may play important roles in the synthesis of large interstellar molecules. In addition, interstellar grains, which are often only of order 10 nm in size, possibly start out as clusters of some sort and subsequently accumulate other atoms. Initial studies of the chemistry and photofragmentation properties of these clusters have begun.

5. Condensed matter physics in penning traps

Daniel Dubin

The experiments which I wish to describe involve trapping a collection of ions or electrons. When cooled to sufficiently low temperatures, these systems exhibit liquid and even crystalline states. At the NBS in Boulder, a cloud of beryllium or mercury ions is confined in a Penning trap [24]. At UCSD, a Malmberg trap (Penning trap made of cylinders) is used to confine high density electron clouds. The similarity of these two efforts is the desire to look at many charged particles confined within the trap (10^2–10^3 ions at Boulder and 10^7–10^{11} electrons at UCSD). These collections of particles have sufficient density and temperature to form pure electron or pure ion plasmas; that is, the Debye length is small compared to the size of the system, so that many of the collective effects that one sees in neutral plasmas can be found in these nonneutral plasmas. For instance, one sees plasma waves, Debye shielding effects, etc.

However, there are also significant differences. Pure electron and pure ion plasmas can be confined indefinitely using only static fields and can come to a thermal equilibrium state. These latter statements depend only on the existence of cylindrical symmetry, which can be achieved experimentally to a high degree of accuracy. This symmetry implies that the

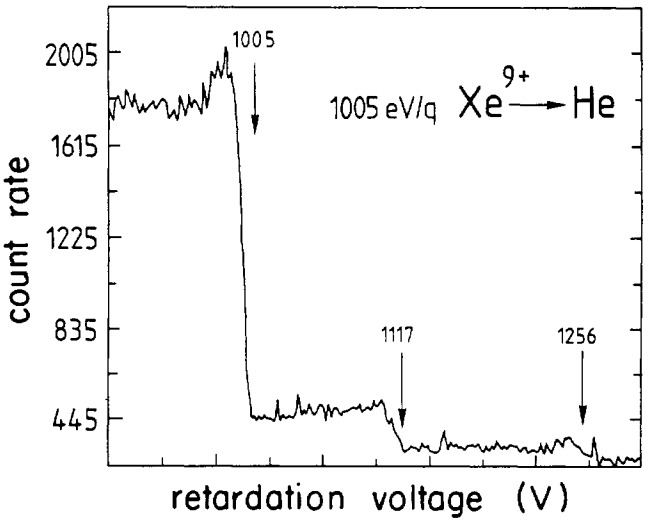

Fig. 2. Ion count rate versus the retardation voltage. The flat part on the left corresponds to the intensity of the primary Xe^{9+} ions, the flat part in the middle to Xe^{8+} ions produced by single charge transfer from He, and the flat part to the right to Xe^{7+} ions produced by double charge transfer from He.

they are decelerated to a few eV just before injection into the trap. In this process, one needs to be concerned that the narrow energy distribution of the recoil ions is not altered. To test for this possibility, we have constructed a retarding field analyzer to measure the recoil ion velocity and obtain a sharp cutoff voltage, thus demonstrating that the narrow recoil ion velocity distribution has not been significantly changed. Figure 2 displays this in a related experiment [17] using our apparatus to yield sharp retarding voltage cutoffs for single and double charge transfer collisions between Xe^{q+} (q = 3 to 12) and helium atoms. The efficiency of the ion transfer system was measured to be about 90%. We hope to do the first storage of recoil ions at the UNILAC this year.

3.3. *Future developments*

First, the experimental apparatus will be used to observe the unique stretched momentum states populated by consecutive polarized charge transfer collisions which are needed for the measurements of the magnetic moment. The technique should work for any charge state ion which can be produced at the UNILAC. Our first candidates will be Ne^{9+} and C^{3+} ions. For a measurement of the magnetic moment of the bound electron, an even isotope with no hyperfine structure will be selected. Extensions to other precision measurements will be possible:

- Measurements of the ground state hyperfine structure of odd-isotope, highly charged hydrogenic ions to test QED and nuclear structure contributions.
- Collision studies involving low energy highly charged ions in a regime where orbiting is predominant.

This work is supported by the National Science Foundation and the Center for Energy and Mineral Resources of Texas A&M University.

4. Laboratory astrophysics with ion traps

Randall D. Knight

Ion traps have proven to be especially useful devices for measuring the physical properties of ions. This is particularly pertinent to low temperature plasmas, such as nebulae, stellar atmospheres, and other objects with energies of the order of eV. These systems consist predominantly of ions in low charge states, and a knowledge of lifetimes, cross-sections, and similar parameters is essential for a detailed understanding of their behavior. Ion traps have become a workhorse of the laboratory astrophysics trade in measuring such quantities. Here, we present an overview of some of the ways in which ion traps have been used in laboratory astrophysics and give some indication as to likely future directions of research. There has been an extensive amount of work done in this field, and the present discussion is by no means exhaustive. The topics which will be considered here are metastable state lifetimes, charge exchange, ion-molecule chemistry, and ion clusters.

Metastable state lifetimes are of interest since the density of astrophysical plasmas is low enough to allow long-lived states to decay radiatively, rather than to undergo collisional relaxation. In fact, comparison of the intensities of forbidden to allowed lines is the primary technique for obtaining plasma densities, and this technique relies upon accurate transition probabilities. In the UV range of 100–200 nm, one finds that 63 of 65 emission lines seen in the solar spectrum are forbidden, most of which are from low charge state ions. Other forbidden lines are seen in nebulae.

A literature search reveals that an impressive number of metastable state lifetimes have been measured in ion traps by several different groups [18]. As summarized in Table II, the measured lifetimes range from tens of μs up to one minute. A variety of ion traps, sources, and techniques have been used, although the most common procedure has been simply to measure the spontaneous decay curve for ions which have been created by electron impact, with some fraction in the metastable state. Measurements of lifetimes longer than 1s employed optical pumping schemes since it is impractical to measure spontaneous decay curves for such long lifetimes.

We anticipate that metastable lifetime work will continue, but most likely with higher charge states. As far as astrophysical interest is concerned, the lower charge state work is

Table II. *Ion trap measured lifetimes. For the decay modes: Inter. E1 — intercombination electric dipole; E2 — electric quadrupole; M1 — magnetic dipole.*

Ion	State	Lifetime	Decay Mode	Type of Trap
Si^{++}	$3s3p\ ^3P_1$	60 μs	Inter. E1	RF
Al^+	$3s3p\ ^3P_1$	300 μs	Inter. E1	RF
Li^+	$1s2s\ ^1S_0$	500 μs	2 photon	Penning
O^{++}	$2s2p^3\ ^5S_2$	1.2 ms	Inter. E1	RF
He^+	$2s\ ^2S_{1/2}$	1.9 ms	2 photon	Penning
N^+	$2s2p^3\ ^5S_2$	4.2 ms	Inter. E1	RF
Xe^{++}	$5p^4\ ^1S_0$	4.5 ms	M1	RF
C^{++}	$2s2p\ ^3P_1$	14 ms	Inter. E1	RF
Kr^{++}	$4p^4\ ^1S_0$	15 ms	M1	RF
Hg^+	$5d^96s^2\ ^2D_{3/2}$	20 ms	E2	Static
Yb^+	$5d\ ^2D_{3/2}$	52 ms	E2	RF
Hg^+	$5d^96s^2\ ^2D_{5/2}$	98 ms	E2	Static
Ar^{++}	$3p^4\ ^1S_0$	110 ms	M1	Static
B^+	$2s2p\ ^3P_1$	115 ms	Inter. E1	Static
Sr^+	$4d\ ^2D_{5/2}$	345 ms	E2	RF
Sr^+	$4d\ ^2D_{3/2}$	395 ms	E2	RF
Cu^+	$3d^94s\ ^1D_2$	510 ms	E2 + M1	Static
Ba^+	$5d\ ^2D_{3/2}$	18 s	E2	RF
Ba^+	$5d\ ^2D_{5/2}$	47 s	E2	RF
Li^+	$1s2s\ ^3S_1$	59 s	M1	RF

canonical angular momentum, defined as

$$P_\theta = \sum_{i=1}^{N} \left(m v_{\theta_i} \varrho_i - \frac{m\Omega}{2} \varrho_i^2 \right), \tag{2}$$

is conserved, where cylindrical coordinates (ϱ, θ, z) are used, Ω is the cyclotron frequency, N is the number of ions, and m the mass. The first term is the kinetic contribution and the second is the vector potential contribution. For strong magnetic fields the latter term dominates and so P_θ is proportional to the mean square cylindrical radius of the plasma, which must therefore remain constant during the evolution of the plasma for the time it is trapped. This means that the plasma can *not* expand. A rigorous computation [25] has shown that a thermal equilibrium does exist, implying for instance that there is no free energy for instabilities. These quiescent plasmas are thus ideal for experiments on waves and transport phenomena.

Another difference relative to neutral plasmas is that pure electron and pure ion plasmas can be cooled to low temperatures without any recombination (no opposite species exists with which to combine). When one reaches a temperature such that the average potential energy per particle, e^2/a (where a is the interparticle spacing), is on the order of kT (where T is the temperature), strong correlation effects become important in the system. In fact, computer simulations for infinite homogeneous noneutral plasmas [26] predict transitions to liquid and crystal states. For values of the order parameter $\Gamma \equiv e^2/akT \ll 1$, we have the above described plasmas. When $\Gamma \gtrsim 2$, the system behaves like a liquid, i.e., it is characterized by damped oscillations in the correlation function. Furthermore, for $\Gamma \gtrsim 170$, one gets a crystalline state. At UCSD, values of Γ range from 1 to 5 for 10^{10} particles. At Boulder, laser cooling techniques on 10^2–10^3 ions produces values of Γ from 10 to 1000, so that the solid phase should be accessible.

Besides making it possible to achieve rather large values of Γ, lasers may be used to great advantage in the determination of various properties of ion clouds, such as density and temperature. Unfortunately, it is much more difficult to diagnose electron plasmas using lasers. This is because the cross-section for laser scattering off of electrons is much smaller than the cross-section for scattering off of internal resonances in ions. However, with such a small number of ions it is not obvious that the ion cloud is in the thermodynamic limit; also, surface effects may be important.

Nevertheless, one advantage of small numbers is that one can do computer simulations of the system in a realistic geometry. It is hoped that these simulations can be compared with the Boulder experiments in the future. I will now discuss some of the results of these simulations, which employ molecular dynamics (MD) and Monte Carlo (MC) techniques.

An important phenomenon, which has been observed in computer studies of infinite homogeneous systems [26], is a phase transition to a b c c crystalline state at $\Gamma \sim 170$. What we observe in our molecular dynamics and Monte Carlo simulations, however, is quite different. We observe the formulation of spheroidal shells; for a spherical cloud with $N = 100$ this occurs at $\Gamma \simeq 140$ (see Fig. 4), and for larger numbers of ions the value of Γ for which shell-formation occurs therefore increases. (A study of this N dependence is underway.) There is negligible mixing of ions from shell to shell, though ions are free to move around on a given shell;

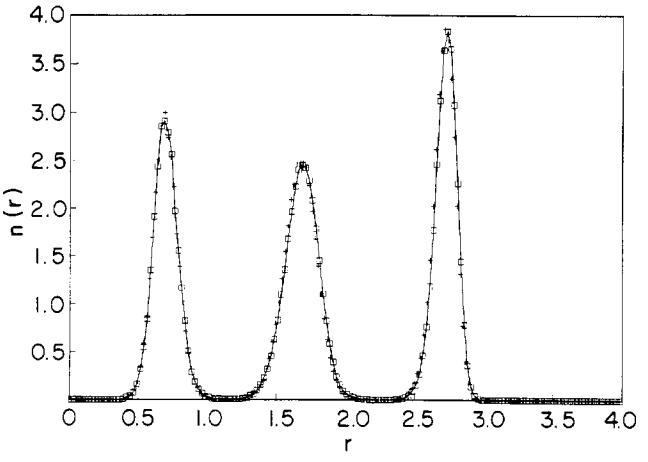

Fig. 4. Density as a function of spherical radius for a spherical ion cloud for $N = 100$. Squares: MD result for $\Gamma = 141 \pm 5\%$. Crosses: MC result for $\Gamma = 141$. Line drawn through squares as an aid to the eye. Distance normalized to a.

this motion is diffusive in nature. Diffusion coefficients have been measured for various values of Γ. For example, for the cloud shown in Fig. 4, we plot in Fig. 5 the mean square change in z, $\langle \delta z^2(t) \rangle$ where z is in the B-field direction, and the mean square change in spherical radius, $\langle \delta r^2(t) \rangle$. The function $\langle \delta z^2(t) \rangle$ is defined as

$$\langle \delta z^2(t) \rangle = \frac{1}{mN} \sum_{i=1}^{N} \sum_{j=1}^{m} [z_i(t + t_j) - z_i(t_j)]^2 \tag{3}$$

where z_i is the z-position of ion i, $t_j - t_{j-1}$ is a constant time and $t \leqslant t_j - t_{j-1}$; there is an analogous definition for $\langle \delta r^2(t) \rangle$. The diffusion coefficient D_z is given by $\langle \delta z^2(t) \rangle = 2D_z t$, similarly for D_r. From Fig. 5, one can see that D_r is essentially zero, while D_z is finite. Thus, the system is crystallized in r, but remains a fluid on each separate shell. This intermediate state between liquid and crystal is due to the inhomogeneity for the system and so is not seen in simulations of infinite homogeneous nonneutral plasmas.

At larger values of Γ, a hexagonal close-packed structure is observed on the outer shells (see Fig. 6). This is similar to the results of Rahman and Schiffer for cylindrical systems [27] on which Dr Schiffer reported at this meeting; however, curvature effects distort the lattice. For $N = 100$, there are 4 ions on the inner shell, 26 on the middle shell and 70 on the outer shell.

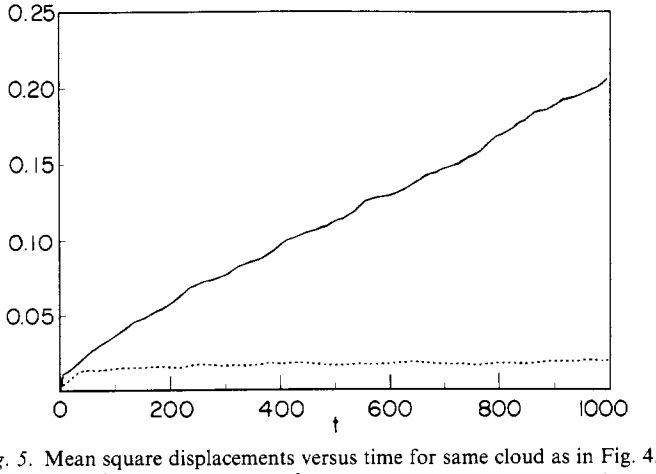

Fig. 5. Mean square displacements versus time for same cloud as in Fig. 4. Solid line: $\langle \delta z^2(t) \rangle$; dotted line: $\langle \delta r^2(t) \rangle$. Distances normalized to a, time to single particle axial bounce frequency.

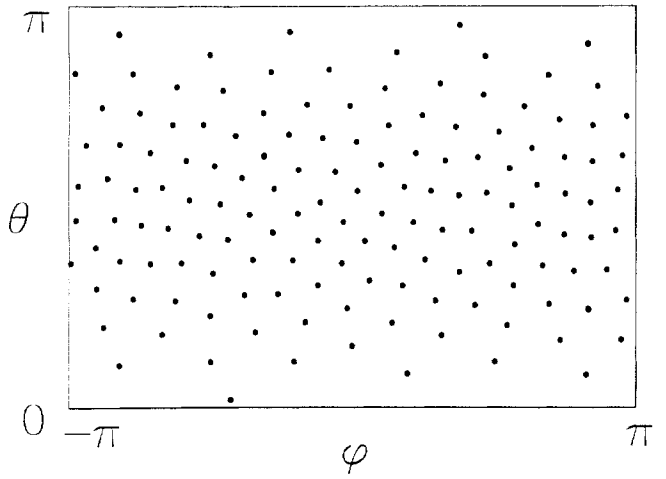

Fig. 6. Polar plot of ion positions in the outer sphere for a spherical plasma with $N = 356$ and $\Gamma = 290 \pm 5\%$; ($\theta = 0$ on the positive z-axis). θ and ϕ are measured in radians.

Now, I want to discuss possible experiments which would test the above predictions. The first experiment is imaging of the plasma using laser fluorescence, presently going on at Boulder. One shines a laser beam through the ion cloud. If spheroidal shells exist, the beam will intersect each shell at two points providing strong fluorescence signals at these separate points. Another way of seeing the crystal structure is to perform Bragg scattering off of the lattice. This difficult experiment is also being attempted at Boulder.

Another experiment suggested by our computer results is a measurement of particle diffusion. This could be measured in a number of ways. For instance, one well known method involves tagging an ion with a laser beam by putting it in a long-lived excited state. The ion reemits after it has diffused some distance through the cloud and so its new position can be measured. If a shell structure has formed, one should see no change in radius of the ion.

Finally, one could try to manipulate the plasma in some way to measure thermodynamic quantities. For instance, one might try an adiabatic expansion of the plasma by lowering the end cap potential V very slowly (compared to all relevant frequencies in the plasma). The plasma will expand along the magnetic field, and the temperature T will change. This change is proportional to the thermodynamic derivative $(\partial T/\partial V)s$ where S is the entropy. Since this derivative is a function of the degree of correlation, one can examine the effects of strong correlation by measuring T vs. V. Note that the derivative involves surface tension effects, which may be important for small systems of ions.

This work is supported by the National Science Foundation under Grant No. PHY87-06358 as well as a grant of computer time from the San Diego Super Computer Center Allocation Committee.

6. Optical traps for neutral particles — New ideas

William D. Phillips

I would like to discuss two ideas for optical trapping that are out of the mainstream of recent development in optical traps. The first idea concerns the possibility of making a feedback trap for atoms — i.e., a scheme for sensing the atom's position and providing an optical force which servos its position to a desired location. Such schemes have long been used to servo the position of macroscopic objects [28, 29] and the question often arises as to whether they can work for single atoms.

Consider a one-dimensional (1-D) version of an optical trap: An atom is irradiated by two independent, counter-propagating laser beams. These exert roughly equal but opposite radiation pressure forces on the atom. We collect the light scattered by the atom and focus it onto a position-sensitive detector. If the detector sees the atom move toward one side, it increases the intensity of the laser beam coming from that side, pushing the atom back toward the center. For a strong optical transition, taking realistic estimates for optical collection and quantum efficiency of detectors, we can expect to see about 10^4 counts/s. For a Poisson statistics-limited signal-to-noise of 10 (presumably sufficient for a good servo) we need 100 counts, or an observation time τ_{obs} of 10^{-2} s to determine where the atom is located. How far does an atom move during the time required to locate it? If the atom is Na laser cooled to the limit, its velocity v_{cl} is about 0.5 m/s, so it moves 0.5 cm. This is a relatively large distance if we wish to confine the atom to a 1 cm region of space. Thus, prospects of a single atom servo trap would seem to be rather poor.

All of this is without the concept of optical molasses [30, 31]. The very strong damping provided by tuning the lasers slightly red of the atomic resonance insures that the motion will be diffusive rather than ballistic as assumed above. For Na in 1-D, the damping time τ_d is about 10 μs. We assume the atom executes a random walk of τ_{obs}/τ_d steps, each step having a length of $v_{cl} \cdot \tau_d$. The mean square distance diffused is $\langle x^2 \rangle = (v_{cl}\tau_d)^2 \cdot (\tau_{obs}/\tau_d)$ or $x_{rms} = (v_{cl}\tau_{obs}) \cdot (\tau_d/\tau_{obs})^{1/2}$. Thus in molasses, the atom goes $(\tau_d/\tau_{obs})^{1/2}$ of the distance it would go ballistically (without molasses). For our case, $\tau_d/\tau_{obs} \approx 10^{-3}$ so the distance diffused in $\tau_{obs} = 10^{-2}$ s is only about 160 μm, a sufficiently small distance that the servo should work.

In three dimensions the situation is not quite as good because the damping time increases by a factor of 3, but it is still quite realistic. Chris Edge has done some detailed analyses which show that it should be possible to construct such a trap [32]. One outstanding question is whether the scheme could work for more than one atom. I don't believe it is possible with the simple geometry presented here, but perhaps a more sophisticated scheme could work.

The second idea I would like to discuss comes from Cohen–Tannoudji's group at Ecole Normale Superieure in Paris. It concerns the trapping of atoms in an optical standing wave. This idea was originally proposed [33] by Letokhov in 1965 even before the idea of laser cooling had been proposed. According to this idea, dipole forces would confine the atoms to the antinodes if the optical frequency were below resonance and to the nodes if above resonance. Once the idea of laser cooling was set forth and the concept of the cooling limit understood, it was realized that such trapping, with a single red-tuned laser frequency, could not be stable: the kinetic energy of the atoms is never much less than the depth of the potential well.

Recently the group at Ecole Normale demonstrated strong cooling in a blue-tuned standing wave [34]. This effect, seemingly paradoxical in view of the usual red-tuned laser cooling, was predicted by Minogen and Serimaa [35]. Its most

graphic explanation is in the dressed atom picture where the atom moves through the hills and valleys of its dressed energy levels. Because it is more likely to undergo radiative decay at the top of a hill than at the bottom of a valley, the atom climbs more than it falls and so it loses kinetic energy [34].

Now, in even more recent experiments, the Ecole Normale group has demonstrated "channeling" – 1-D confinement of atoms to the nodes of a blue-tuned standing wave. The channels seen by the atoms are the time average of its dressed-state potentials, and are periodically varying in space, with minima at the nodes. Interestingly, this channeling is quite effective even in the absence of cooling, although cooling can further improve the channeling. This channeling represents a realization of Letokhov's original idea.

Because the channeled atom is localized near a node of the standing wave, it spends relatively little of its time in the excited state. Therefore, its spontaneous emission and radiative heating are minimized. This reduces the chance that an atom will acquire enough energy to jump out of the channel. Viewed in the dressed atom picture, an atom spends most of its time in a valley of a dressed potential, only occasionally decaying radiatively to a peak from which it can escape to an adjacent channel. Furthermore, the atom is often moving slowly enough that it can decay back to a valley and remain trapped in the same channel before it can move into another channel. As a result, the residence time in a channel can be quite long, perhaps as long as milliseconds.

Channelization also occurs for red-detuning, but here everything works against the atom's staying in a given channel. Atoms are channeled near antinodes, so heating is maximized. Furthermore, the strong damping is reversed, causing the atoms to be quickly boiled out of the channels.

It is particularly interesting to speculate as to the effect of extending this localization in a blue-tuned standing wave to three dimensions. Then atoms would be confined to potential wells having an extent less than a half wavelength. They would occasionally hop to adjacent wells. This would result in a random walk of step size $\lambda/2$ (0.3 μm for Na) and time between steps of milliseconds. Compared to the random walk in ordinary red-tuned molasses – step size $> 20\lambda$ and time between steps of tens of microseconds – this blue-tuned lattice of potential wells would result in considerably longer confinement times, perhaps 10^6 s for a 1 cm diffusion time.

7. Magnetic traps for neutral particles

Greg Lafyatis

We have heard at this conference of remarkably precise spectroscopy, both rf and optical, that is being done in ion traps. I will discuss the possibility of using similar techniques to do precision spectroscopy in magnetic-type neutral atom traps. Recent advances in such traps make this discussion especially timely. We are now able to trap 10^9 sodium atoms for over 2 min and cool them to mK temperatures [36].

By way of introduction to the neutral trapping field, I would like to mention briefly some aspects of the magnetic trapping work ongoing at M.I.T. Figure 7 depicts some of the experimental features of our trap. Atoms with electronic spins oriented parallel to the magnetic field see a potential energy $U = \mu_B|\vec{B}|$ and may be trapped near a local minimum of the magnetic field. Our axial field near the bottom of the trap is also shown in Fig. 7. Radial confinement of the atoms

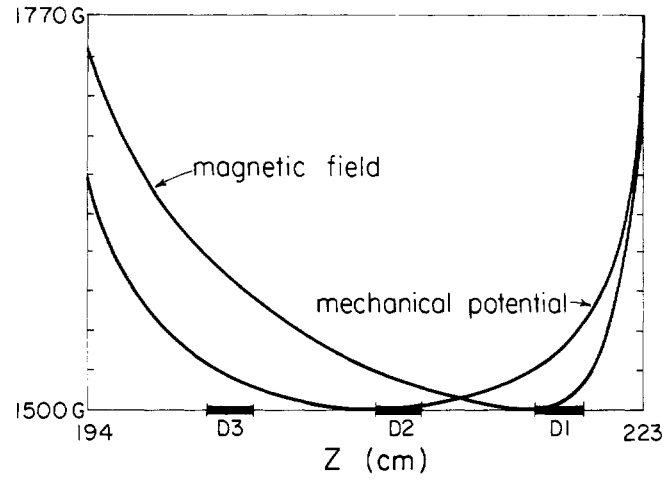

Fig. 7. Magnetic neutral particle trap. Both the magnetic field potential and the total mechanical potential seen by the atoms are shown. The detector positions are labeled D1, D2, and D3.

is limited to a cylinder 4 cm in diameter and 25 cm long. Laser beams are used to Doppler cool the atoms in the trap to ~2 mK. The atoms are diagnosed *via* fluorescence observed in detectors at positions labelled D1, D2, and D3 in Fig. 7. Gravity's effect – which will turn out to be an important problem for doing precision spectroscopy in magnetic neutral traps – is readily seen in our present experiment. The trap axis is vertical and thus, the total mechanical potential that the atoms see is the magnetic potential plus the gravitational potential. We observe that this effect shifts the trap minimum by 10 cm (see Fig. 7) from the magnetic field minimum.

Lets consider doing precision spectroscopy in a trap similar to this one. We have in mind determining frequency to high precision either for use in standards or for fundamental physics experiments. Neutral traps share important virtues that ion traps have demonstrated for precision spectroscopy: cold samples with greatly reduced first and second order Doppler shift broadening and long interrogation times. Neutral traps offer the following additional advantages:

- Since atoms interact much less than ions, it should be possible to use much larger samples. Significant gains in signal-to-noise may be had.
- Some important species – e.g., hydrogen and anti-hydrogen – happen to be neutral.
- Neutral species tend to have transitions more accessible to laser excitation (i.e., longer wavelength) than ions.

The major disadvantage in doing precision spectroscopy in magnetic-type neutral traps is that different states of an atom have different interaction energies with the trapping fields. Consequently, the transition energy between two states will be inhomogeneously broadened as atoms with different translational energies sample different fields. One solution is to work with a very cold atomic sample and bias the trap to a value where the atomic transition is field independent to first order. As cooler samples are obtained, weaker traps may be used and the broadening will be reduced. In what follows, we will consider a sample that has been cooled to the temperature which corresponds to a single recoil photon (there are several schemes in the literature for doing this [37]) – for sodium, this limit is 2 μK. Note that at this temperature, the second order Doppler shift is entirely negligible: $\delta f/f \approx 10^{-20}$.

Gravity limits how far this scheme may be implemented. The trapping field cannot be arbitrarily weak in that it must hold the atoms up against gravity. In fact, as in Fig. 7, the bottom of the net mechanical potential is that point in the field where the magnetic field gradient exactly compensates gravity: 4.5 G/cm for sodium. In fact, atoms confined to a volume with height h (in cm) will sample a field variation of $4.5h$ Gauss in addition to that from the field simply needed to trap the atoms. The transition will be correspondingly broadened and shifted; because we are working at a field independent point for the transition, the motion of the atoms in the trap will *not* average the shift in the transition frequency from this field variation. We may minimize this effect by making h as small as possible, but again, there are limits, since a major reason for working with neutrals is to increase signal-to-noise by using lots of particles. For a given number of particles, we can only decrease the size of our trap to the point that interactions among the particles become important. Hence, gravity requires us to trade off trap size for numbers of particles in order to reduce the inhomogeneous broadening of the transition while retaining good signal-to-noise. Moreover, there is little reason to try to cool atoms much below $kT = mgh$ (corresponding to a temperature of 30 μK for Na with $h = 1$ mm). In what follows, we consider a trap containing 10^6 atoms in a cylindrical volume with a horizontal axis, 1 cm long and 0.1 mm in diameter.

Now, lets examine some specific transitions. First, we will consider r.f. transitions. For comparison purposes, today's best r.f. frequency standards, cesium beam clocks, have a fractional accuracy (roughly speaking) of a part in 10^{13}. Transitions between magnetic hyperfine states within the ground state manifold of an alkali system are suitable sources for precision r.f. spectroscopy. As a favorable case, consider the 1,550 MHz transition between the upper two states of the ground state manifold of ^{87}Rb which is field independent to first order at 37,300 G. As the upper level is a "cycling" level for the $5s$–$5p$ transition, by exciting and monitoring the transition, we derive the shelving amplification factor: a change of one atom from the lower to the upper state of the r.f. transition will change the detected fluorescence signal by thousands of photons per second. It may be assumed that the signal-to-noise ratio, then, is given by the shot noise due to the finite number of atoms, n, in the sample. With an interrogation time of 100 seconds and 10^6 atoms, we find a fractional linewidth, $\delta f/f \approx 10^{-12}$, with sufficient signal-to-noise to split the line to one part in 1000. The limit on the measurement's precision from the broadening and shift of the resonance due to the gradient of the B-field across the trap is on the order of 2×10^{-13}. If this shift and broadening can be independently measured – by looking at a field dependent transition, for example – it should be possible to determine the r.f. transition frequency to $(\delta f/f)(S/N)^{-1} = 10^{-15}$.

The fractional precision of r.f. spectroscopic measurements is limited by the large interrogation times required to make a high Q measurement. Despite significant present day technical obstacles, it is expected that superior frequency standards may be had by going to optical frequencies. Which atomic systems are suitable for measurement in neutral traps? We go to the periodic table and require that a candidate atom have both a long lived "clock" transition and a "cycling" transition for probing the clock transition in a shelving arrangement. The following systems are found suitable: H, Ag, and several of the rare earths. Of the rare earths, at least five have the following similar features:

- There are long-lived "clock" transitions in the infrared (with lifetimes of 10–1000 seconds).
- They have weak cycling transitions in the infrared.
- They have very large ground and excited state manifolds which will require attention to avoid optical pumping.

Consider erbium as a typical example. It has a ground state manifold of 104 magnetic hyperfine states. "Cycling" transitions exist at 1300 nm, 840 nm, and 631 nm. A 2.1 μ ($\tau \geqslant 100$ s) "clock" transition – which must be probed using first order "Doppler-free" techniques – is field independent at $B = 1750$ G. In the trap described above, the inhomogeneous broadening from the field gradient across the trap gives a line $Q \approx 10^{15}$ (requiring a 1 s interrogation time). If this broadening can be independently characterized, the signal-to-noise is adequate to split the line and measure the frequency to a part in 10^{18}. This compares very favorably with ion trap frequency standards under consideration [38].

Although fraught with technical difficulties, an intriguing possibility is to do precision spectroscopy on the $1s$–$2s$ transition in atomic hydrogen (this may be probed *via* the $1s$–$2p$ transition). The field dependence of the upper states in the respective manifolds is so nearly identical – they depart from being exactly parallel principally due to the so called "relativistic correction" terms [39] – that it is not necessary (nor possible) to work at a first order field independent point. The natural lifetime of the state yields a line $Q \approx 2 \times 10^{15}$. One may use 10^{10} to 10^{12} particles in a much larger volume; in this case, the atoms will average the magnetic field gradient necessary to hold them against the gravitational field (because the variation in the transition frequency is linear in the field variation) and the transition will only be broadened by the trapping potential. For atoms cooled to 1 μK, this would lead to a broadening/shift of the transition corresponding to ≈0.3 Hz. Beyond making an excellent frequency standard, the transition may also be used in an ultra high precision measurement of the Rydberg. Finally, if one could obtain sufficiently cold anti-hydrogen, it would be possible to compare the Rydberg in anti-hydrogen to that in hydrogen and thereby test CPT. Of course, in the process, we would no doubt learn how gravity affects anti-hydrogen atoms.

References

1. Van Dyck, Jr., R. S., Wineland, D. J., Ekstrom, P. A. and Dehmelt, H. G., Appl. Phys. Lett. **28**, 446 (1976); Gabrielse, G., Phys. Rev. A. **27**, 2277 (1983).
2. Van Dyck, Jr., R. S., Schwinberg, P. B. and Dehmelt, H. G., Phys. Rev. D **34**, 722 (1986); and in *New Frontiers in High Energy Physics* (Plenum, N.Y., 1978) p. 159.
3. Van Dyck, Jr., R. S., Schwinberg, P. B. and Dehmelt, H. G., Phys. Rev. Lett. **59**, 26 (1987).
4. Schwinberg, P. B., Dehmelt, H. G., and Van Dyck, Jr., R. S., Phys. Lett. **81A**, 119 (1981).
5. Van Dyck, Jr., R. S., Moore, F. L., Farnham, D. L., and Schwinberg, P. B., Rev. Sci. Instrum. **57**, 593 (1986).
6. Green, G. L., Kessler, Jr., E. G., Deslattes, R. D., and Börner, H., Phys. Rev. Lett. **56**, 819 (1986).
7. Lippmaa, E., Pikver, R., Suurmaa, E., Past, J., Puskar, J., Koppel, I., and Tammik, A., Phys. Rev. Lett. **54**, 285 (1985).
8. Gabrielse, G., Fei, X., Helmerson, K., Rolston, S. L., Tjoelker, R., Trainor, T. A., Kalinowsky, H., Haas, J. and Kells, W., Phys. Rev. Lett. **57**, 2504 (1986).
9. Hu, C. S., *et al.*, Nucl. Phys. **A254**, 403 (1975); Roberson, P. L., *et al.*,

Phys. Rev. **C16**, 1945 (1977); and Roberts, B. L., Phys. Rev. D. **17**, 358 (1978).
10. These are reviewed by Kinoshita, T., in the Proceedings of the 1986 Conference on Precision Electromagnetic Measurements, NBS Gaithersburg, Maryland, June 23–27 (1986).
11. Schuessler, H. A., Hyperfine Interactions **24–26**, 119 (1985).
12. Grotch, H. and Hegstrom, R. A., Phys. Rev. **A4**, 59 (1971).
13. Kienle, P., Report GSI-86-43 (1986).
14. O, C. S. and Schuessler, H. A., J. Phys. D.: Appl. Phys. **14**, 953 (1981).
15. Salin, A., J. Physique **45**, 671 (1984).
16. Brieger, M. and Schuessler, H. A., Physica Scripta [this issue] (1987).
17. Chen, S., Schuessler, H. A., Trebus, U., Zhang, J. and Mann, R., Bull. Am. Phys. Soc. Series II Vol **31**, No. 5, 1003 (1986).
18. See Smith, P. L., Johnson, B. C., Kwong, H. S., Parkinson, W. H. and Knight, R. D., Physica Scripta **T8**, 88 (1984); Prior, M. H., Phys. Rev. **A30**, 3051 (1984); Gerz, Ch., Hilberath, Th. and Werth, G., Z. Physik **D5**, 97 (1987) and references therein.
19. See Church, D. A., in "Atomic Physics 9," p. 137 (Edited by R. S. Van Dyck, Jr., and E. N. Fortson), World Scientific Publishing Company, Singapore, (1984) and references therein.
20. Prior, M. H., Marrus, R. and Vane, C. R., Phys. Rev. **A28**, 141 (1983).
21. Church, D. A., Kenefick, R. A., Burns, W. S., O, C. S., Holmes, R., Huldt, S., Berry, S., Breinig, M., Elston, S., Rozet, J.-P., Sellin, I. A., Taylor, D. and Thomas, B., Phys. Rev. Lett. **49**, 643 (1983).
22. See Barlow, S. E., Luine, J. A., and Dunn, G. H., Inter. J. Mass Spectrom. and Ion. Proc. **74**, 97 (1986) and references therein.
23. Knight, R. D., Walch, R. A., Foster, S. C., Miller, T. A., Mullen, S. L. and Marshall, A. G., Chem. Phys. Lett. **129**, 331 (1986).
24. Bollinger, J. and Wineland, D., Phys. Rev. Lett. **53**, 348 (1984).
25. Prasad, S. and O'Neil, T. M., Phys. Fluids **22**, 278 (1979).
26. Pollock, E. and Hansen, J., Phys. Rev. **A8**, 3110 (1973); Slattery, W., Doolan, G. and DeWitt, H., Phys. Rev. **A21**, 2087 (1980).
27. Rahman, A. and Schiffer, J., Phys. Rev. Lett. **57**, 1133 (1986).
28. Holmes, F. T., Rev. Sci. Instrum. **8**, 444 (1937).
29. Ashkin, A., Science **210**, 1081 (1980).
30. Chu, S. *et al.*, Phys. Rev. Lett. **55**, 48 (1985).
31. Phillips, W., Prodan, J. and Metcalf, H., J. Opt. Soc. Am. **B2**, 1751 (1985).
32. Edge, C., University of Virginia, private communication (1985).
33. Letokhov, V. S., Pis'ma Zh. Eksp. Teor. Fiz **7**, 348 (1968) [JETP Lett. **7**, 272 (1968).]
34. Aspect, A. *et al.*, Phys. Rev. Lett. **57**, 1688 (1986).
35. Minogen, V. G., and Serimaa, O. T., Opt. Commun. **30**, 373 (1979).
36. Bagnato, V. S., Lafyatis, G. P., Martin, A. G., Raab, E. L., Ahmad-Bitar, R. N., and Pritchard, D. E., Phys. Rev. Lett. **58**, 2194 (1987).
37. Pritchard, D. E., Phys. Rev. Lett. **51**, 1336 (1983).
38. David Wineland, private communication.
39. Bethe, H. A. and Salpeter, E. E., "Quantum Mechanics of One and Two Electron Atoms," Springer, Berlin (1957).